ARTICLE IN PRESS

Available online at www.sciencedirect.com

SCIENCE DIRECT®

Journal of Organometallic Chemistry 689 (2004) 1418–1424

Journal of Organometallic Chemistry

www.elsevier.com/locate/jorganchem

The counterion influence on the CH-activation of methane by palladium(II) biscarbene complexes – structures, reactivity and DFT calculations ☆

Thomas Strassner *, Michael Muehlhofer, Alexander Zeller, Eberhardt Herdtweck, Wolfgang A. Herrmann

Anorganisch-chemisches Institut der Technischen Universität München, Lichtenbergstrasse 4, 85747 Garching, Germany

Received 17 November 2003; accepted 4 February 2004

Abstract

Novel bridged palladium(II) biscarbene complexes with different counterions are reported: 1,1′-dimethyl-3,3′-methylene-4-diimidazolin-2,2′-diylidene palladium(II) bischloride (**1**) and bis(trifluoroacetate) (**2**) have been synthesized in good yields. Both complexes are active in the catalytic conversion of methane to methanol and show comparable activities to previously published NHC-catalysts. The results of the single-crystal X-ray structure determination of 1,1′-dimethyl-3,3′-methylene-4-diimidazolin-2,2′-diylidene palladium(II) bischloride (**1**) and 1,1′-dimethyl-3,3′-methylene-4-diimidazolin-2,2′-diylidene palladium (II) bis(trifluoroacetate) **2** confirmed the structural similarity to the known corresponding palladium bromide and iodide complexes. Since free 1,1′-dimethyl-*R*-3,3′-methylene-4-diimidazolin-2,2′-diylidene are only available in low yields these compounds have been synthesized via the bromide complex, exchanging the counterion by $AgCF_3COO$ or by exchanging the counterion of the imidazolium salt by NH_4PF_6.

Keywords: CH-activation; Palladium; N-heterocyclic carbene; Methane; Catalysis

1. Introduction

Novel metal complexes of imidazoline-2-ylidenes have recently been shown to be extremely versatile and stable catalysts for a wide range of reactions including C–C-coupling reactions [1–3], olefin metathesis [4–7], hydroformylation [8,9], polymerisation reactions [10,11] and most recently CH-activation [12]. The key for this development have been improved synthetic methods for the preparation of N-heterocyclic carbene (NHC) complexes, which have been reported in recent reviews [13,14].

The unusual high thermal stability combined with the surprising resistance to acidic media allowed their use for the activation and conversion of methane to methanol in trifluoroacetic acid (CF_3COOH) [12]. But only the 1,1′-dimethyl-3,3′-methylene-4-diimidazolin-2,2′-diylidene palladium(II) dibromide (**3**) showed activity, while the 1,1′-dimethyl-3,3′-methylene-4-diimidazolin-2,2′-diylidene palladium(II) diiodide **4** did not activate methane. To investigate this counterion dependence of the reaction we synthesized the complexes 1,1′-dimethyl-3,3′-methylene-4-diimidazolin-2,2′-diylidene palladium(II) bischloride (**1**) and 1,1′-dimethyl-3,3′-methylene-4-diimidazolin-2,2′-diylidene palladium(II) bistrifluoroacetate **2** (Scheme 1).

Metal acetates allow the direct synthesis of NHC complexes without isolation of the free carbene, palladium(II)acetate in wet dimethyl sulphoxide (DMSO) at elevated temperatures deprotonates the imidazolium salt. Even methylene bridged bisimidazolium salts can be converted to the corresponding biscarbene complexes in high yields (85–90%) [10,11,15]. This route is very useful in cases where the metal acetates are easily available. Alternatively, the corresponding metal halides

☆ Presented at the New York ACS meeting (INOR-547).

* Corresponding author. Tel.: +49-89-289-13174; fax: +49-89-289-13473.

E-mail address: thomas.strassner@ch.tum.de (T. Strassner).

0022-328X/$ - see front matter © 2004 Elsevier B.V. All rights reserved.
doi:10.1016/j.jorganchem.2004.02.013

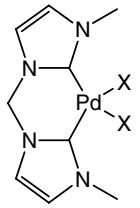

1: X = Cl
2: X = CF_3COO
3: X = Br
4: X = I

Scheme 1. Palladium complexes with NHC-ligands.

and sodium acetate can be employed which was recently shown in the case of platinum biscarbene complexes [16]. When palladium acetate is used, the counterion of the carbene complex is provided by the imidazolium salt. Accordingly, for the synthesis of the bisbromide **3** and bisiodide **4** complexes the bromide and iodide salts can be used. Since methylene bridged bisimidazolium chloride salts are not known, new synthetic pathways for the parent complexes had to be found. In the case of weaker coordinating anions (like in complex **2**) exchange with silver salts is the preferred pathway [10,17] (see Scheme 2).

Theoretical calculations and especially density functional theory calculations have recently shown to be very helpful in evaluating properties and reactions of transition metal complexes [18]. Therefore, Becke3LYP/6-311+G(d,p) [19–23] calculations have been used to evaluate the stability of the complexes and of potential intermediates.

We report the synthesis of novel palladium NHC complexes, their solid-state structures as well as their activities in the catalytic methane activation together with DFT-calculations on the palladium halide bond strengths.

2. Experimental

2.1. General procedures

Solvents of 99.5% purity were used throughout this study. Palladium(II) chloride (98%) was received from ABCR. All other chemicals were obtained from common suppliers and used without further purification.

^1H, ^{13}C and ^{19}F NMR spectra were recorded on a JEOL JNM GX 400 spectrometer. The spectra were either referenced internally using the resonances of the solvent (^1H, ^{13}C) or externally to CCl_3F (^{19}F). Elemental analyses were performed by the microanalytical laboratory in our institute. Mass spectra were recorded on a Finnigan MAT 90 spectrometer.

1,1′-Dimethyl-3,3′-methylene-diimidazolium dibromide and 1,1′-dimethyl-3,3′-methylene-4-diimidazolin-2,2′-diylidene palladium(II) dibromide were prepared according to the literature procedures [15,16].

2.2. Synthesis of 1,1′-dimethyl-3,3′-methylene-4-diimidazolin-2,2′-diylidene palladium(II) dichloride (*1*)

262 mg 1,1′-dimethyl-3,3′-methylene-diimidazolium bishexafluorophosphate **5** (0.56 mmol), 65 mg sodium chloride (1.12 mmol), 99 mg palladium(II) chloride (0.56 mmol) and 152 mg sodium acetate (1.12 mmol) were dissolved in 10 ml DMSO and stirred for 2 h at RT,

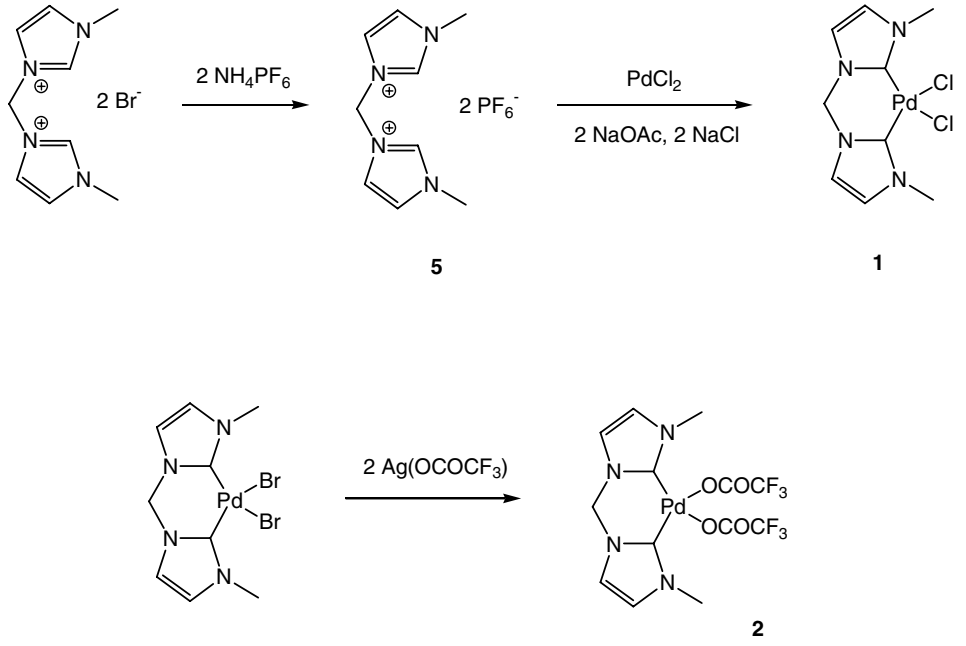

Scheme 2. Synthesis of bridged Pd–NHC complexes.

followed by 5 h at 60 °C. Subsequently, the solution was heated to 90 °C for 2 h. After the removal of the solvent, the residue was washed with water and THF yielding a white powder. The crude product was recrystallized from DMSO/methanol (104 mg, 53%). ^{1}H NMR (400 MHz, DMSO-d_6): δ 7.56 (s, 2H, NCH), 7.30 (s, 2H, NCH), 6.24 (s, 2H, NCH_2N), 3.91 (s, 6H, CH_3). ^{13}C NMR (100.5 MHz, DMSO-d_6): δ 157.1 (NCN); 123.0 (NCH); 121.9 (NCH); 62.3 (CH_2); 37.7 (CH_3). MS(EI) m/z: 318 $[M–Cl]^+$, 282 $[M–2Cl]^+$.

2.3. Synthesis of 1,1′-dimethyl-3,3′-methylene-4-diimidazolin-2,2′-diylidene palladium(II) bis(trifluoroacetate) (2)

297 mg 1,1′-dimethyl-3,3′-methylene-4-diimidazolin-2,2′-diylidene palladium(II) dibromide (0.67 mmol) and 295 mg silver trifluoroacetate (1.34 mmol) were suspended in 10 ml acetonitrile and stirred for 8 h at 60 °C. The solution was filtered off and the solvent was removed in vacuo to give a white solid (300 mg, 88%). ^{1}H NMR (400 MHz, DMSO-d_6): δ 7.65 (d, 2H, NCH), 7.40 (d, 2H, NCH), 6.32 (s, 2H, NCH_2N), 3.75 (s, 6H, CH_3). ^{13}C NMR (100.5 MHz, DMSO-d_6): δ 159.1 (q, $^2J_{C,F} = 32$ Hz, CO); 148.5 (NCN); 123.8 (NCH); 121.9 (NCH); 116.3 (q, $^1J_{C,F} = 294$ Hz, CF_3); 62.0 (CH_2); 36.5 (CH_3). ^{19}F NMR (376.2 MHz, DMSO-d_6): δ -69 (s, CF_3). Anal. Calc. for $C_{13}H_{12}F_6N_4O_4Pd$: C, 30.70; H, 2.38; N, 11.01. Found: C, 30.87; H, 2.48; N, 11.16%.

2.4. Synthesis of 1,1′-dimethyl-3,3′-methylene-diimidazolium bis hexafluorophosphate (5)

To a solution of 676 mg 1,1′-dimethyl-3,3′-methylene-diimidazolium dibromide (2 mmol) in 5 ml of water, 684 mg ammonium hexafluorophosphate (4.2 mmol) in 5 ml water are added. A white precipitate is formed which is filtered off and dried in vacuo, yielding a white solid (740 mg, 79%). ^{1}H NMR (400 MHz, acetonitrile-d_3): δ 8.76 (s, 2H, NCHN), 7.57 (s, 2H, NCH), 7.43 (s, 2H, NCH), 6.38 (s, 2H, NCH_2N), 3.86 (s, 6H, CH_3). ^{13}C NMR (100.5 MHz, acetonitrile-d_3): δ 157.1 (NCN); 123.0 (NCH); 121.9 (NCH); 62.3 (CH_2); 37.7 (CH_3). Anal. Calc. for $C_9H_{14}N_4F_{12}P_2$: C, 23.10; H, 3.01; N, 11.97. Found: C, 22.85; H, 2.85; N, 11.71%.

2.5. Structure determination of compound 1

Crystal data and details of the structure determination are presented in Table 1. Table 2 summarizes selected bond distances and bond angles. Suitable single crystals for the X-ray diffraction study were grown from slow diffusion of methanol into a concentrated solution of **1** in DMSO (see Fig. 1). A clear colorless needle ($0.05 \times 0.05 \times 0.36$ mm) was stored under perfluorinated ether, transferred in a Lindemann capillary, fixed and

Table 1
Crystal data and summary of intensity data collection and structure refinement of compounds **1** and **2**

	1	**2**
Formula	$C_9H_{12}Cl_2N_4Pd$	$C_{13}H_{12}F_6N_4O_4Pd$
Formula weight	353.55	508.69
Color/shape	Colorless/needle	Colorless/fragment
Space group	*Pbca* (No. 61)	$P2_1/c$ (No. 14)
a (Å)	14.8373(2)	8.4301(1)
b (Å)	9.9459(1)	9.0115(1)
c (Å)	16.5181(2)	22.8833(4)
β (°)	90	96.3687(7)
V (Å^3)	2437.58(5)	1727.67(4)
Z	8	4
ρ_{calcd} (g cm^{-3})	1.927	1.956
μ (mm^{-1})	1.938	1.166
Diffractometer	Nonius kappa-CCD	Nonius kappa-CCD
λ (Å) (Mo Kα)	0.71073	0.71073
T (K)	123	173
Reflections integrated	56 175	32 960
Independent reflections (all data)	2221	3163
Observed reflections ($I > \sigma(I)$)	2036	2857
Parameters refined	147	329
R_1 (observed/all data)	0.0367/0.0416	0.0237/0.0284
wR_2 (observed/all data)	0.0875/0.0904	0.0525/0.0557
Goodness-of-fit (observed/all data)	1.107/1.107	1.083/1.083
Residual electron density (e Å^{-3})	3.21[a]/−0.39	0.62/−0.41

[a] The high residual electron density is judged as a mathematical artefact based on an imperfect absorption correction.

Table 2
Characteristic bond lengths (Å) and bond angles (°) for compounds **1** and **2**

	1	**2**	$\mathbf{1}_{calc}$	$\mathbf{2}_{calc}$
Pd–C1	1.966(4)	1.954(3)	2.019	1.988
Pd–C6	1.973(4)	1.955(3)	2.019	2.004
Pd–Cl1	2.3782(10)		2.396	
Pd–Cl2	2.3727(10)		2.396	
Pd–O1		2.078(2)		2.097
Pd–O3		2.084(2)		2.095
C5–N2	1.462(5)	1.452(4)	1.456	1.452
C5–N3	1.456(5)	1.455(3)	1.456	1.458
C1–Pd–C6	83.81(16)	84.25(11)	86.0	86.69
C1–Pd–Cl1	176.58(12)		174.64	
C1–Pd–Cl2	90.57(12)		90.58	
C6–Pd–Cl1	94.19(11)		90.58	
C6–Pd–Cl2	172.66(11)		174.64	
Cl1–Pd–Cl2	91.20(3)		92.54	
C1–Pd–O1		178.48(9)		176.54
C1–Pd–O3		96.79(9)		91.33
C6–Pd–O1		94.52(9)		91.47
C6–Pd–O3		178.27(9)		174.84
O1–Pd–O3		84.46(7)		90.27
N2–C5–N3	108.2(3)	108.9(2)		110.08

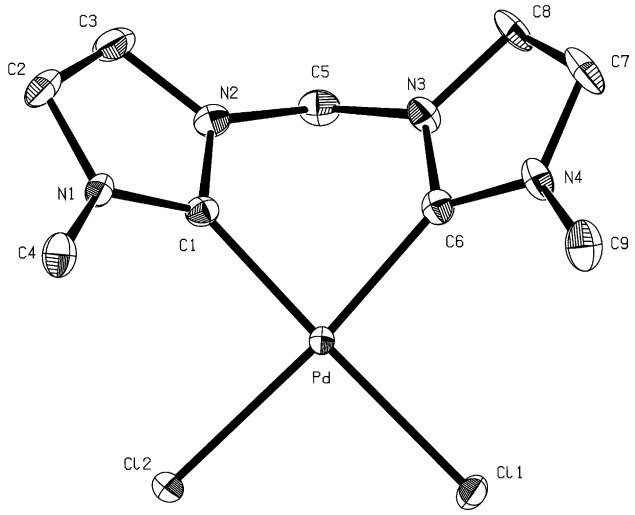

Fig. 1. ORTEP style plot of the solid-state structure of compound **1**. Thermal ellipsoids are drawn at the 50% probability level. The hydrogen atoms are omitted for clarity.

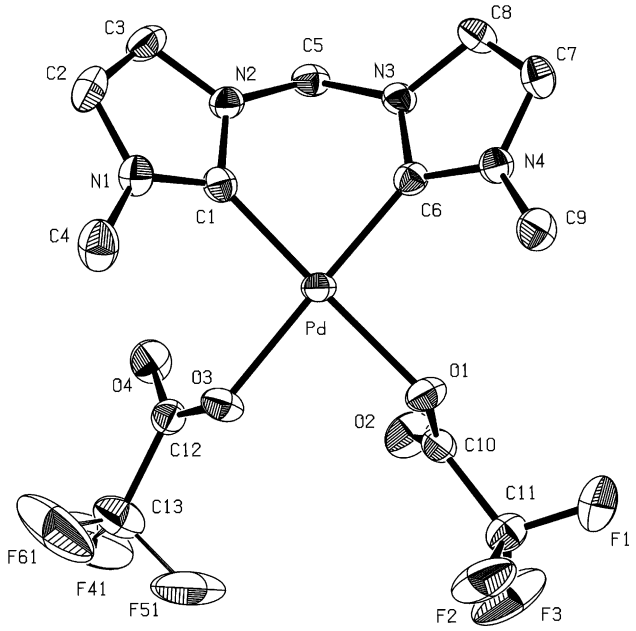

Fig. 2. ORTEP style plot of the solid-state structure of compound **2**. Thermal ellipsoids are drawn at the 50% probability level. For clarity, the hydrogen atoms are omitted and only one orientation of the disordered CF_3 group at C13 is shown.

sealed. Preliminary examination and data collection were carried out on an area detecting system (kappa-CCD; Nonius) at the window of a rotating anode (Nonius; FR591) and graphite monochromated Mo Kα radiation ($\lambda = 0.71073$ Å). The unit cell parameters were obtained by full-matrix least-squares refinement of 2551 reflections. Data collection was performed at 123 K within a θ-range of $2.47° < \theta < 25.33°$. Nine data sets were measured in rotation scan modus with $\Delta\varphi/\Delta\Omega = 2.0°$. A total number of 56 175 intensities were integrated. Raw data were corrected for Lorentz, polarization, decay and absorption effects. After merging ($R_{int} = 0.053$) a sum of 2221 independent reflections remained and were used for all calculations. The structure was solved by a combination of direct methods and difference Fourier syntheses. All non-hydrogen atoms were refined with anisotropic displacement parameters. All hydrogen atoms were calculated in ideal positions riding on the parent carbon atoms. Full-matrix least-squares refinements with 147 parameters were carried out by minimizing $\sum w(F_o^2 - F_c^2)^2$ with SHELXL-97 weighting scheme and stopped at shift/err < 0.001. Neutral atom scattering factors for all atoms and anomalous dispersion corrections for the non-hydrogen atoms were taken from International Tables for Crystallography. All calculations were performed on an Intel Pentium II PC, with the STRUX-V system, including the programs PLATON, SIR-92, and SHELXL-97 m[24–30].

2.6. Structure determination of compound **2**

Crystal data and details of the structure determination are presented in Table 1. Table 2 summarizes selected bond distances and bond angles. Suitable single crystals for the X-ray diffraction study were grown from slow diffusion of diethylether into a concentrated solution of **2** in acetonitrile (see Fig. 2). A clear colorless fragment (0.10×0.13 0.30 mm) was stored under perfluorinated ether, transferred in a Lindemann capillary, fixed and sealed. Preliminary examination and data collection was carried out on an area detecting system (kappa-CCD; Nonius) at the window of a rotating anode (Nonius; FR591) and graphite monochromated Mo Kα radiation ($\lambda = 0.71073$ Å). The unit cell parameters were obtained by full-matrix least-squares refinement of 3369 reflections. Data collection was performed at 173 K within a θ-range of $1.79° < \theta < 25.52°$. Seven data sets were measured in rotation scan modus with $\Delta\phi/\Delta\Omega = 1.0°$. A total number of 32960 intensities were integrated. Raw data were corrected for Lorentz, polarization, decay and absorption effects. After merging ($R_{int} = 0.034$) a sum of 3163 independent reflections remained and were used for all calculations. The structure was solved by a combination of direct methods and difference Fourier syntheses. All non-hydrogen atoms were refined with anisotropic displacement parameters. All hydrogen atoms were found in the difference Fourier maps and refined freely. Full-matrix least-squares refinements with 329 parameters were carried out by minimizing $\Sigma w(F_o^2 - F_c^2)^2$ with SHELXL-97 weighting scheme and stopped at shift/err < 0.001. A disorder over two positions (59:41) of the CF_3 group bound at C13 could be resolved clearly. Neutral atom scattering factors for all atoms and anomalous dispersion corrections for the non-hydrogen atoms were taken from International Tables for Crystallography. All calculations were

performed on an Intel Pentium II PC, with the STRUX-V system, including the programs PLATON, SIR-92, and SHELXL-97 [24–30].

2.7. Density functional theory calculations

All calculations were performed with GAUSSIAN-98 [19]. The density functional hybrid model Becke3LYP [20–23] was used together with the valence triple-ζ basis set 6-311+G(d,p). Palladium was treated by a small core Hay–Wadt VDZ effective core potential (ECP) [31]. No symmetry or internal coordinate constraints were applied during optimizations. All reported intermediates were verified as true minima by the absence of negative eigenvalues in the vibrational frequency analysis.

Approximate free energies were obtained through thermochemical analysis of the frequency calculation, using the thermal correction to Gibbs free energy as reported by GAUSSIAN-98. This takes into account zero-point effects, thermal enthalpy corrections, and entropy. All energies reported in this paper, unless otherwise noted, are free energies at 298 K and 1 atm. Frequencies remain unscaled.

3. Results and discussion

3.1. Preparation and spectroscopic data of complexes 1 and 2

The direct preparation of the palladium biscarbene dichloride (**1**) from the corresponding imidazolium chloride salt was not possible since attempts to synthesize the latter have not been successful. Using the common procedure methylene chloride and methyl imidazole did not react even at temperatures above 150 °C in a pressure tube. Thus, an imidazolium salt with weakly coordinating anions (PF_6^-) was used for the synthesis with in situ replacement by chloride. This salt **5** can easily be prepared by exchange of the counterions of bisimidazolium dibromide with ammonium hexafluorophosphate in water [32]. Palladium chloride was chosen as the metal precursor and sodium acetate as the base. Heating of **5** with $PdCl_2$ and NaOAc led to the partial formation of palladium black during the reaction which is evidence of the presence of unstable intermediates. This was circumvented by the addition of two equivalents of sodium chloride. In this manner **1** was obtained in good yield as a white solid. The crude product contains small amounts of the corresponding bishexafluorophosphate complex which was detected by ^1H (the corresponding BF_4^- complex is described in the literature [10]) and ^{31}P NMR, but no complex with mixed counterions. This anion scrambling had also previously been observed during the synthesis of platinum biscarbene complexes [16].

The bistrifluoroacetate complex **2** was obtained by replacement of the bromide anions of complex **3** with silver trifluoroacetate in acetonitrile in good yields as a white powder. ^1H NMR signals show a shift of the N-heterocyclic carbene (NHC) backbone resonances to lower field which is indicative for a higher positive partial charge in the ligand. The ^{13}C NMR spectrum shows the characteristic trifluoroacetate signals with ^{13}C–^{19}F coupling. By ^{19}F NMR spectroscopy only one signal at -69 ppm for both CF_3 groups is observed.

Crystals suitable for a X-ray investigation of **1** were obtained from DMSO/methanol, crystals of **2** were grown from acetonitrile/ether. Details of the solid-state structure determination are given in Table 1, important geometrical parameters are shown in Table 2.

Complexes **1** and **2** are isotype to **3** [33] and **4** [34] with a bowl shaped NHC ligand. The Pd–carben–C distances in the dichloride **1** (1.966(4) and 1.973(4) Å) and bistrifluoroacetate complex **2** (1.954(3) and 1.955(3) Å) are only slightly shorter than in the dibromide **3** (1.971(5) and 1.983(5) Å) or diiodide **4** (1.988(7) and 1.989(8) Å) complex. The trifluoroacetate counterions in **2** are equivalent within the margin of error. Interestingly, molecules of **2** form dimers in the solid state which are stabilized by C–H···O interactions between carbonyl oxygen atoms of the trifluoroacetate anion and C–H bonds of the methylene bridge.

3.2. Catalytic results for the methane activation

The activity of complexes **1**–**3** in the catalytic conversion of methane to the methyl ester was tested in order to elucidate the influence of the counterion, keeping in mind that the corresponding iodide complex **4** showed no activity [12]. The reactions were conducted in the presence of palladium catalysts **1**–**3** (0.21 mmol) and $K_2S_2O_8$ (21 mmol) in a mixture of trifluoroacetic acid and its anhydride (40 ml/30 ml). Compared to previous experiments [12], a higher fraction of anhydride was used in this study which led to a slightly smaller activity, but it reduced the harshness of the reaction conditions drastically thereby improving the durability of the autoclave material. A methane pressure of 30 bar at a temperature of 90 °C was used since these reaction

Table 3
Results of catalysis experiments (reaction conditions: 0.21 mmol catalyst, 5.70 g (21 mmol) potassium peroxodisulfate, 30 bar methane, 20 h reaction time, $T = 90$ °C, 40 ml trifluoroacetic acid/30 ml trifluoroacetic acid anhydride)

Entry	Catalyst	TON[a]
1	**1**	24
2	**2**	21
3	**3**	24
4	**3** + 10 equivalents KBr	No reaction

[a] Determined by GC analysis.

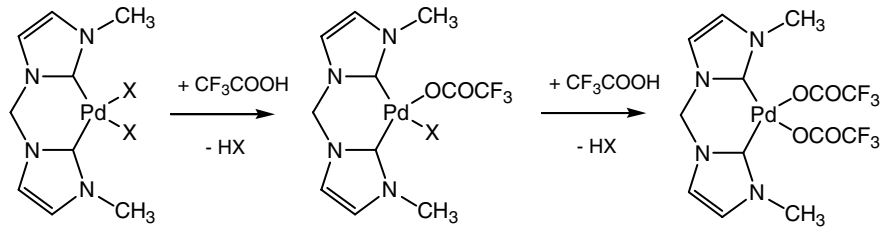

Scheme 3. Anion-exchange process.

conditions have previously given the highest yield of methyl ester [12]. The results are given in Table 3.

It can be concluded that the influence of the anion is rather small, the activity of complexes **1**–**3** is comparable within the margin of error. On the other hand, this is to be expected in the case that the counterion does not participate in the catalytic cycle. According to DFT calculations, the initial exchange of both bromide anions to trifluoroacetates consumes 20.4 kcal/mol. The experimental results suggest that this step is rather fast at 90 °C and no significant deactivation by re-coordination of bromide occurs during the reaction. On the other hand, a high concentration of bromide anions in the reaction solution leads to a termination of the activity of complex **3** (Table 3, Entry 4) since reco-ordination of a bromide anion stops the catalytic cycle.

3.3. Results of DFT calculations

To investigate the bond strength of the different anions, density functional theory calculations were undertaken. The agreement between the experimentally observed geometric parameters and the calculated ones is excellent (Table 2). The reaction product observed after the catalytic reaction is CF_3COOCH_3, no halogenated products (e.g. CH_3Br) were found in the GC traces. A possible reaction pathway is the replacement of the anions by trifluoroacetic acid as shown in Scheme 3 followed by coordination of the methane, electrophilic substitution, oxidation and reductive elimination of CF_3COOCH_3.

The initial halogen exchange might make the difference and therefore this process was calculated for the different halogens F^-, Cl^-, Br^- and I^-. Only for fluorine an exergonic reaction is predicted, the replacement of all other halogens is endergonic (Table 4). The calculated free energies for both steps increase from fluorine to iodine. For all anions but fluorine the first replacement requires significantly more free energy than the second step.

These results predict that the replacement of all halogens can proceed under the reaction conditions. The energy difference between the bromide and iodide ligands is not large enough to explain the inactivity of catalyst **4**. We are currently investigating the full reaction profile including the transition states, which will provide more insight than the ground state results.

Table 4
B3LYP/6-311+G(d,p) calculated free energies (kcal/mol) for the replacement of the halogen ligands by trifluoroacetic acid

	First replacement	Second replacement	Overall reaction
F	−2.8	+1.2	−1.6
Cl	+11.1	+3.5	+14.7
Br	+14.1	+6.3	+20.4
I	+16.8	+9.2	+26.0

4. Conclusion

We present the synthesis and structural characterization of new palladium biscarbene complexes, which are active in the CH-activation of methane. The influence of the counterion is not as big as originally thought, the activities are comparable between the various [Pd(Me–NHC-CH_2-NHC-Me)X_2] complexes described here.

While for $X = I^-$ no activation could be observed, all other ligands tested have shown comparable high activity. The solid-state structures confirm the similarity of the molecular geometries which seem to be independent on the counterion. DFT calculations predict the most endergonic reaction for the iodine complex **4**, but the calculated difference of 5.6 kcal/mol to the bromine complex **3** is not large enough to explain the experimental result. We are therefore currently investigating the reaction kinetics by identifying the rate determining step and the counterion influence on this transition state.

5. Supporting information available

Crystallographic data (excluding structure factors) for the structures reported in this paper have been deposited with the Cambridge Crystallographic Data Centre as supplementary publication Nos. CCDC-224335 (**1**) and CCDC-224334 (**2**). Copies of the data can be obtained free of charge on application to CCDC, 12 Union Road, Cambridge CB2 1EZ, UK (fax: +44-1223-336-033; e-mail: deposit@ccdc.cam.ac.uk).

Acknowledgements

We are grateful for the financial support by Süd-Chemie Int. and for the computer time provided by the Leibniz-Rechenzentrum Munich.

References

[1] W.A. Herrmann, M. Elison, J. Fischer, C. Koecher, G.R.J. Artus, Angew. Chem., Int. Ed. Engl. 34 (1995) 2371.
[2] V.P.W. Böhm, T. Weskamp, C.W.K. Gstöttmayr, W.A. Herrmann, Angew. Chem. Int. Ed. 39 (2000) 1602.
[3] S. Caddick, F.G.N. Cloke, G.K.B. Clentsmith, P.B. Hitchcock, D. McKerrecher, L.R. Titcomb, M.R.V. Williams, J. Organomet. Chem. 617-618 (2001) 635.
[4] T. Weskamp, W.C. Schattenmann, M. Spiegler, W.A. Herrmann, Angew. Chem. Int. Ed. 37 (1998) 2490.
[5] T. Weskamp, F.J. Kohl, W. Hieringer, D. Gleich, W.A. Herrmann, Angew. Chem. Int. Ed. 38 (1999) 2416.
[6] M. Scholl, S. Ding, C.W. Lee, R.H. Grubbs, Org. Lett. 1 (1999) 953.
[7] M.S. Sanford, J.A. Love, R.H. Grubbs, J. Am. Chem. Soc. 123 (2001) 6543.
[8] W.A. Herrmann, J.A. Kulpe, W. Konkol, H. Bahrmann, J. Organomet. Chem. 389 (1990) 85.
[9] W.A. Herrmann, C.W. Kohlpaintner, Angew. Chem. 105 (1993) 1588.
[10] M.G. Gardiner, W.A. Herrmann, C.-P. Reisinger, J. Schwarz, M. Spiegler, J. Organomet. Chem. 572 (1999) 239.
[11] J. Schwarz, E. Herdtweck, W.A. Herrmann, M.G. Gardiner, Organometallics 19 (2000) 3154.
[12] M. Muehlhofer, T. Strassner, W.A. Herrmann, Angew. Chem., Int. Ed. Engl. 41 (2002) 1745.
[13] T. Weskamp, V.P.W. Bohm, W.A. Herrmann, J. Organomet. Chem. 600 (2000) 12.
[14] W.A. Herrmann, Angew. Chem., Int. Ed. Engl. 41 (2002) 1290.
[15] J. Schwarz, V.P.W. Bohm, M.G. Gardiner, M. Grosche, W.A. Herrmann, W. Hieringer, G. Raudaschl-Sieber, Chem. Eur. J. 6 (2000) 1773.
[16] M. Muehlhofer, T. Strassner, E. Herdtweck, W.A. Herrmann, J. Organomet. Chem. 660 (2002) 121.
[17] W.A. Herrmann, J. Schwarz, M.G. Gardiner, M. Spiegler, J. Organomet. Chem. 575 (1999) 80.
[18] M. Torrent, M. Sola, G. Frenking, Chem. Rev. (Washington, DC) 100 (2000) 439.
[19] M.J. Frisch, G.W. Trucks, H.B. Schlegel, G.E. Scuseria, M.A. Robb, J.R. Cheeseman, V.G. Zakrzewski, J.A. Montgomery, R.E. Stratmann, J.C. Burant, S. Dapprich, J.M. Millam, A.D. Daniels, K.N. Kudin, M.C. Strain, O. Farkas, J. Tomasi, V. Barone, M. Cossi, R. Cammi, B. Mennucci, C. Pomelli, C. Adamo, S. Clifford, J. Ochterski, G.A. Petersson, P.Y. Ayala, Q. Cui, K. Morokuma, D.K. Malick, A.D. Rabuck, K. Raghavachari, J.B. Foresman, J. Cioslowski, J.V. Ortiz, A.G. Baboul, B.B. Stefanov, G. Liu, A. Liashenko, P. Piskorz, I. Komaromi, R. Gomperts, R.L. Martin, D.J. Fox, T. Keith, M.A. Al-Laham, C.Y. Peng, A. Nanayakkara, C. Gonzalez, M. Challacombe, P.M.W. Gill, B. Johnson, W. Chen, M.W. Wong, J.L. Andres, C. Gonzalez, M. Head-Gordon, E.S. Replogle, J.A. Pople, GAUSSIAN-98: Revision A.7, Gaussian, Inc., Pittsburgh, PA, 1998.
[20] C. Lee, W. Yang, R.G. Parr, Phys. Rev. B 37 (1988) 785.
[21] S.H. Vosko, L. Wilk, M. Nusair, Can. J. Phys. 58 (1980) 1200.
[22] P.J. Stephens, F.J. Devlin, C.F. Chabalowski, M.J. Frisch, J. Phys. Chem. 98 (1994) 11623.
[23] A.D. Becke, J. Chem. Phys. 98 (1993) 5648.
[24] Data Collection Software for Nonius kappa-CCD devices, Delft, The Netherlands, 1997.
[25] Z. Otwinowski, W. Minor, Methods Enzymol. 276 (1997) 307.
[26] A.J.C. Wilson (Ed.), International Tables for Crystallography, vol. C, Kluwer Academic Publisher, Dordrecht, The Netherlands, 1992; Tables 6.1.1.4 (pp. 500–502), 4.2.6.8 (pp. 219–222), 4.2.4.2. (pp. 193–199).
[27] G.R.J. Artus, W. Scherer, T. Priermeier, E. Herdtweck, STRUX-V: A Program System to Handle X-Ray Data, TU München, Garching, Germany, 1997.
[28] G.M. Sheldrick, SHELXL-97, University of Göttingen, Göttingen, Germany, 1998.
[29] A.L. Spek, PLATON, Utrecht University, Utrecht, The Netherlands, 2001.
[30] A. Altomare, G. Cascarano, C. Giacovazzo, A. Guagliardi, M.C. Burla, G. Polidori, M. Camalli, J. Appl. Crystallogr. 27 (1994) 435.
[31] P.J. Hay, W.R. Wadt, J. Chem. Phys. 82 (1985) 299.
[32] K.M. Lee, J.C.C. Chen, I.J.B. Lin, J. Organomet. Chem. 617-618 (2001) 364.
[33] E. Herdtweck, M. Muehlhofer, T. Strassner, Acta Crystallogr., Sect. E 59 (2003) m970.
[34] W.A. Herrmann, V.P.W. Bohm, C.-P. Reisinger, J. Organomet. Chem. 576 (1999) 23.